Supporting information

Ag supraparticles with 3D hotspots to actively capture molecules for surface enhanced Raman scattering sensitive detection

Mingrui Zhu,[a,b] Guoliang Zhou,[a,b] Ronglu Dong,[b] Pan Li,[b*] Liangbao Yang[b*]
a. University of Science & Technology of China, Anhui, Hefei 230026, China.
b. Anhui Province Key Laboratory of Medical Physics and Technology, Institute of Health and Medical Technology, Hefei Institutes of Physical Science, Chinese Academy of Sciences, Hefei 230031, China.

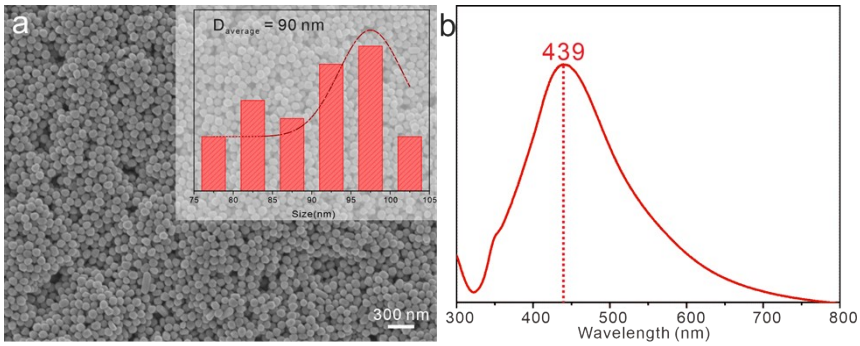

Figure S1. Characterization of Ag nanoparticles. (a) SEM characterization and size distribution of Ag nanoparticles. (b) UV-Vis spectra of Ag nanoparticles.

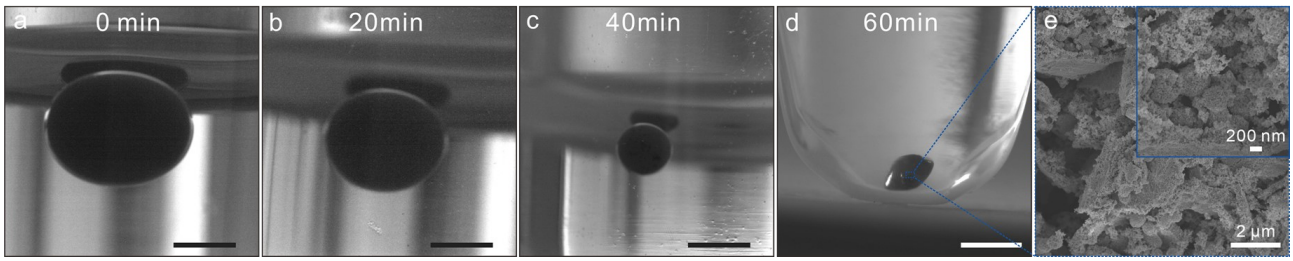

Figure S2. The shrinkage process of Cit Au NPs colloidal. (a-d) A high-speed camera was used to observe the shrinkage process of the sodium citrate-modified Au NPs colloids in the organic phase under ultrasound conditions (the scale bar is 2 mm). (e) SEM image of the final morphology formed from sodium citrate-modified Au NPs.

Figure S3. The shrinkage process of PVP Au NPs colloidal. (a-d) A high-speed camera was used to observe the shrinkage process of PVP-modified Au NPs colloids in the organic phase under ultrasound conditions (the scale bar is 2 mm). (e) SEM image of the final morphology formed from PVP-modified Au NPs.

Figure S4. The shrinkage process when organic phase was chloroform. (a-d) The shrinkage process of citrate stabilized Ag colloids under ultrasonic conditions was observed with a high-speed camera using chloroform as organic phase (the scale bar is 2 mm).

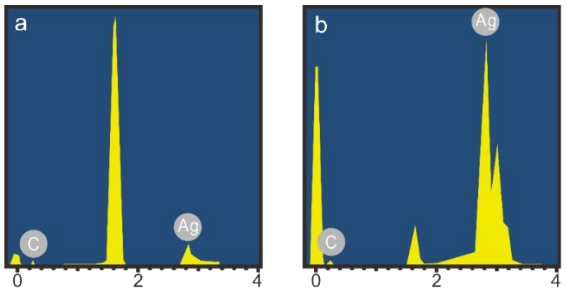

Element	Weight percentage	atomic percent
C	13.01	57.32
Ag	86.99	42.68

Element	Weight percentage	atomic percent
C	2.03	15.71
Ag	97.97	84.29

Figure S5. Comparison of surface EDS spectrometry analysis of supraparticles and sol after natural evaporation (a) EDS diagram after natural drying. (b) EDS diagram of 3D supraparticle.

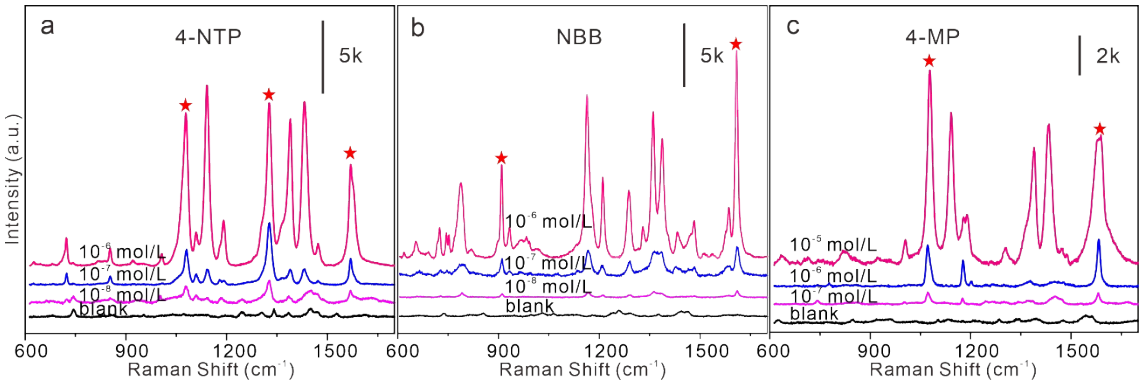

Figure S6. SERS performance measurements of different molecules on 3D supraparticles (a) 4-NTP (4-

Nitrothiophenol); (b) NBB (2-Nitrobenzyl bromide); (c) 4-MP (4-Mercaptohenol).

Table S1. Characteristics, chemical bonds and vibration modes of molecules

Molecule	Characteristic	Chemical bond	Vibrational mode
MG[1]	High toxicity and high redidue, Prohibited drugs for aquaculture	1619 cm^{-1} 1298 cm^{-1}	Ring C-C streching
		1396 cm^{-1}	N-phenyl stretching
		773 cm^{-1}	C-H out-of-plane bending vibration
MB[2]	Antidotes for cyanide and oxidation-reduction indicators	1642 cm^{-1}	Ring C-C stretching vibration
		1420 cm^{-1} 1357 cm^{-1}	C-N stretching
		1184 cm^{-1}	C-H bending vibration
		664 cm^{-1}	C-C-C deformation in plane
6-MP[3]	Antitumor drugs	1307 cm^{-1}	N-C stretching vibration
		1110 cm^{-1}	S-H stretching vibration
		814 cm^{-1}	C-S-H deformation vibration
4-NTP[4]	Probe molecules for studying electrochemical and photochemical reaction mechanisms	1078 cm^{-1}	C-H bending vibration
		1327 cm^{-1}	NO_2 symmetric stretching
		1569 cm^{-1}	C=C stretching vibration
NBB[5]	Bactericidal, antifungal and anti-inflammatory	908 cm^{-1}	Ring C-C respiration
		1608 cm^{-1}	NO_2 Antisymmetric vibration
4-MP[6-7]	Antibacterial, mold inhibiting and antiseptic	1078 cm^{-1}	C–C stretching
		1590 cm^{-1}	Ring stretching vibration

References in the supporting information

1. Zhou, B. B.; Mao, M.; Cao, X. M.; Ge, M. H.; Tang, X. H.; Li, S. F.; Lin, D. Y.; Yang, L. B.; Liu, J. H., Amphiphilic Functionalized Acupuncture Needle as SERS Sensor for In Situ Multiphase Detection. *Anal Chem* **2018,** *90* (6), 3826-3832.
2. Hussain, S.; Nisar, A.; Karim, S.; Yu, Y. L.; Liu, Y. G.; Sun, H. Y.; Zafar, A.; Hussain, S. Z.; Ahmad, M., Tuning the SERS Capabilities of ZnO Nanowire Arrays Functionalized with Au Quantum Dots for Highly Sensitive Detection of Methylene Blue. *Chemistryselect* **2023,** *8* (19).
3. Pannico, M.; Musto, P., SERS spectroscopy for the therapeutic drug monitoring of the anticancer drug 6-Mercaptopurine: Molecular and kinetic studies. *Appl Surf Sci* **2021,** *539*.

4. Sarhan, R. M.; Koopman, W.; Pudell, J.; Stete, F.; Rössle, M.; Herzog, M.; Schmitt, C. N. Z.; Liebig, F.; Koetz, J.; Bargheer, M., Scaling Up Nanoplasmon Catalysis: The Role of Heat Dissipation. *J Phys Chem C* **2019,** *123* (14), 9352-9357.
5. Wang, Y. H.; Du, Y.; Huang, X.; Wu, X. X.; Zhang, Y. X.; Yang, S.; Chi, Y. G. R., Carbene-Catalyzed Reductive Coupling of Nitrobenzyl Bromide and Nitroalkene via the Single-Electron-Transfer (SET) Process and Formal 1,4-Addition. *Org Lett* **2017,** *19* (3), 632-635.
6. Wang, W. K.; Zhang, L. M.; Li, L.; Tian, Y., A Single Nanoprobe for Ratiometric Imaging and Biosensing of Hypochlorite and Glutathione in Live Cells Using Surface-Enhanced Raman Scattering. *Anal Chem* **2016,** *88* (19), 9518-9523.
7. Zhao, L. Z.; Hu, Y. L.; Li, G. K.; Zou, S. Y.; Ling, L. S., Chemical-Chemical Redox Cycle Signal Amplification Strategy Combined with Dual Ratiometric Immunoassay for Surface-Enhanced Raman Spectroscopic Detection of Cardiac Troponin I. *Anal Chem* **2023,** *95* (45), 16677-16682.